

Methods for quantifying rail seat loads and a review of previous experimentation

Brandon J Van Dyk^{1,2}, Andrew J Scheppe¹, J Riley Edwards¹,
Marcus S Dersch¹ and Christopher PL Barkan¹

Proc IMechE Part F:
J Rail and Rapid Transit
2016, Vol. 230(3) 935–945
© IMechE 2015
Reprints and permissions:
sagepub.co.uk/journalsPermissions.nav
DOI: 10.1177/0954409715569862
pif.sagepub.com



Abstract

A railroad sleeper and fastening system is composed of many unique parts that, when assembled, attempt to distribute train wheel loads through the system without damaging the components while providing a safe running surface and track geometry for trains to operate on. In order to evaluate the health of the sleeper and fastening system, there are many areas that need to be examined to ensure that key limit states are not exceeded. One key area of concern is the sleeper rail seat, specifically the load magnitude applied to this surface. There are many different metrics to evaluate the rail seat load, and this report will compare these to determine which should be used given different operating and infrastructure conditions. A sample calculation for each methodology was completed in order to compare how the methods differ, and to more fully understand the strengths and limitations of each methodology. These calculations were completed both with a static load and dynamic load, as the individual approaches account for dynamic loads in a variety of ways. For the purpose of this report, these calculations were completed assuming a concrete sleeper infrastructure. The goal of this paper is to provide an evaluation of the existing rail seat load calculation methodologies to improve current concrete sleeper and fastening system design standards through the application of mechanistic design principles.

Keywords

Concrete sleepers, rail seat, wheel load, design standard

Date received: 26 August 2014; accepted: 30 December 2014

Load quantification objectives

The performance of concrete sleepers and fastening systems is largely dependent on the type and magnitude of the loads that travel through the track superstructure. Although a qualitative understanding of these loads is useful in interpreting fastening system component interactions and resulting failure modes, quantifying these loads is critical to determining the demands each component must withstand. There have been many efforts to quantify wheel loads and limited research investigating how these loads transfer to the underlying infrastructure. However, there is no clear understanding of how the load is distributed after passing from the wheel/rail interface through the rail and into the fastening system and rail seat. A better understanding of the load path needs to be obtained, as well as its distribution to the rail seat, and ultimately its path through the ballast to the subgrade. To better evaluate current designs of the track structure and move forward with offering recommendations for improvements to those designs based on mechanistic practices, Rail Transportation and Engineering Center (RailTEC) researchers have

conducted research and a review of the available literature to quantify the loads travelling through each component as they pass through each interface of the concrete sleeper and fastening system.

Overview of the wheel loading environment

The discussion of the loading environment must begin by distinguishing between, static, quasi-static, dynamic and impact loads. The static load is the load of the rail vehicle at rest, as if it were being weighed on a scale. The quasi-static load is “a low-frequency oscillation superimposed over the static dead weight of the train vehicle at the wheel-rail interface.”¹ More simply, the quasi-static load can be

¹Rail Transportation and Engineering Center (RailTEC), University of Illinois at Urbana-Champaign, IL, USA

²Vossloh Fastening Systems, Chicago, IL, USA

Corresponding author:

Andrew J Scheppe, Newmark Civil Engineering Laboratory, University of Illinois, 205 N. Mathews Avenue, Urbana, IL 61801, USA.

Email: scheppe1@illinois.edu

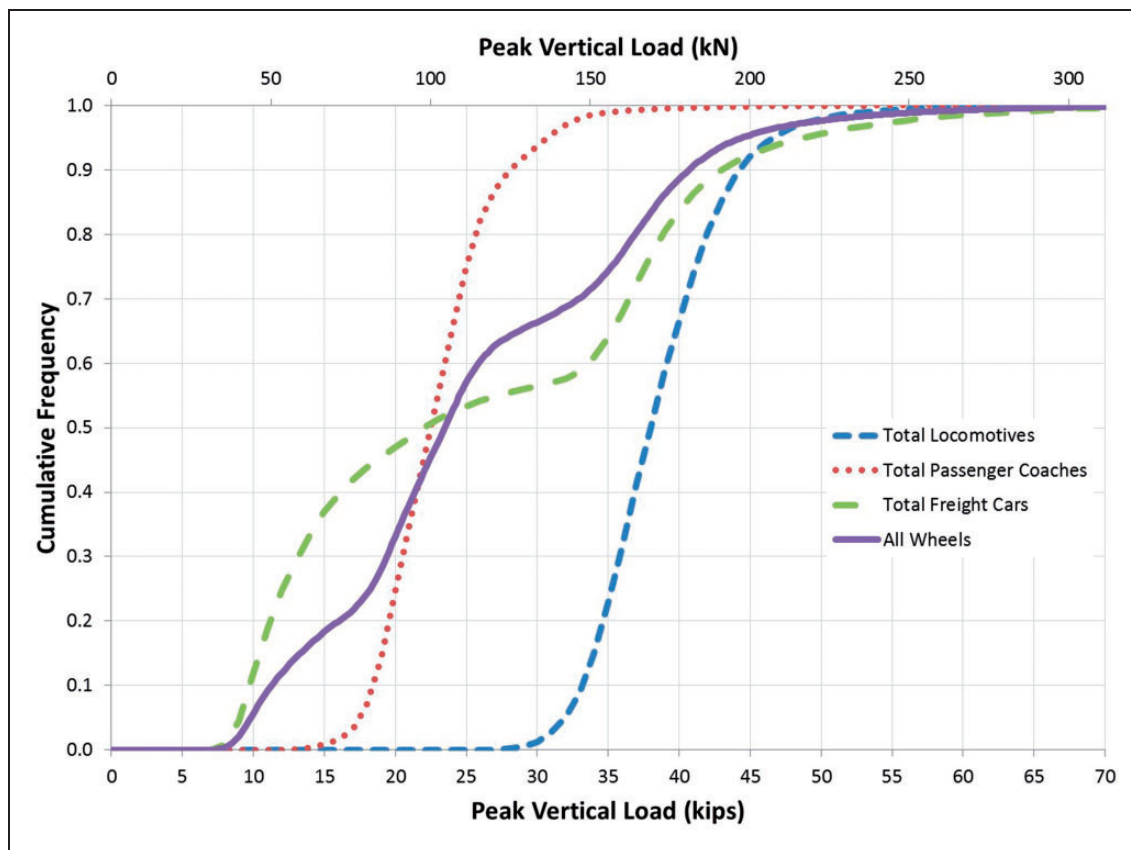


Figure 1. Cumulative frequency of peak vertical loads at Edgewood, Maryland (November 2010).

considered as the combined static load and effect of the static load at speed², independent of time. Dynamic loads are loads due to high-frequency effects of the wheel/rail load interaction, considering track component response and involving inertia, damping, stiffness and mass, and are more complex to quantify. They are characterized by high-frequency load inputs that are dependent on time. The impact load, which often creates the highest loads seen in the track structure, is created by track and wheel irregularities, the most familiar being a flat spot on a wheel. These impacts create high-frequency, short-duration loads that travel through the infrastructure and may cause significant damage. Although these distinctions regarding static and dynamic loads can be applied worldwide, their magnitudes may vary significantly across continents due to a variety of factors.

The operating environment in North America is unique when compared with those of the rest of the world, given the frequent co-existence of passenger traffic and heavy-axle freight traffic on shared infrastructure. As enthusiasm for and operation of new high-speed intercity passenger service grows, it must do so while sharing infrastructure with the existing freight railways for most routes. One of the many challenges facing shared use infrastructure is the performance of critical components that were largely designed for slower-moving, heavy-axle freight trains. To better understand the loading applied to

the infrastructure, the University of Illinois at Urbana-Champaign (UIUC) has acquired significant data from wheel impact load detector (WILD) sites throughout the US from both Amtrak and Union Pacific Railroad.

These data provide insight into the varied loading distributions at representative sites throughout North America. Specific loading properties such as peak vertical load, peak lateral load, and speed are captured through the use of strain gauge instrumentation, and these data are graphed and analyzed by creating various distributions and determining relationships between them. Figure 1 shows 1 month of data that depicts a typical cumulative distribution of locomotive, freight car, and passenger coach peak vertical wheel loads when about 50% of the wheels are related to freight traffic and 50% of the wheels are related to passenger service. The figure shows varied load levels for multiple traffic types travelling over shared infrastructure.^{3,4}

The WILD data also provide information regarding lateral loads, however, because the site is constructed on tangent track the lateral loads do not frequently exceed 5 kips toward the gauge or field side of the rail. To monitor more significant lateral loads in curved sections of track, an instrumented wheel set (IWS) can be utilized. IWS measurements on US coal routes have produced lateral loads up to 31 kips (138 kN) toward the field side of track.⁵

However, it may be possible for even higher lateral loads to occur in areas with non-optimal rail profiles, friction management techniques, track condition or wheel condition.⁶

Longitudinal forces in the track must also be considered. They most often occur because of thermal expansion or contraction of the rail and locomotive tractive effort or braking. Thermal forces in the rail can cause failures resulting in very serious consequences. Significant longitudinal forces can also be generated due to wheel/rail contact. In fact, with proper support conditions, four head-end freight locomotives and a loaded train can generate longitudinal forces in excess of 225 kips (1001 kN).⁷

Investigation and comparison of rail seat load calculation methodologies

Introduction. An important part of railway track structural analysis is understanding the path of the load as it travels through the rail car's suspension system, into the rail, onto the sleepers, and down into the track substructure (ballast and subgrade). It is widely accepted that a wheel load being applied to the rail is then distributed over several sleepers both in front of and behind the location of the wheel, even when it is located directly above a single sleeper.⁸ An exception to this distribution might be in the case of a hanging sleeper, where there is little-to-no support beneath the sleeper, and the entire wheel load is supported by adjacent sleepers. Using specially designed field instrumentation, axle loads can be measured as they pass over a given section of track, thus capturing the overall input load into the track structure. The difficulty lies in understanding the distribution of these axle loads to individual sleepers at the interface of the rail pad and the concrete rail seat area. The importance of understanding this loading lies in the fact that deterioration of the concrete surface at this interface has been identified, and is believed to be a result of a crushing mechanism.⁹ Concrete sleeper deterioration at the rail seat can also be caused by the abrasion mechanism; localized high pressures with relative displacements can cause increased strain on cement particles, leading to deterioration.¹⁰

In order to gain a better understanding of the load path from the wheel and into the rail as it is applied to the sleeper, an investigation of various rail seat load calculation methodologies was undertaken. The methods discussed are some of what currently exist to calculate, or estimate, the loading conditions present at the rail seat of a concrete sleeper. The three methods presented are means of calculating the magnitude of a rail seat load in terms of the total force applied to the rail seat area, and do not relay any information on the pressure or distribution of this load. They consist of methods used by the American Railway Engineering and Maintenance-of-way Association (AREMA), and

equations developed and/or used by Arnold Kerr, and Arthur Newell Talbot. The UIC Standards and Australian Standards also contain rail seat load prediction equations, and are frequently referenced throughout the international railway infrastructure community.^{2,11} The methods will be compared analytically, and the various parameters that impact each method will be discussed and compared. After a brief discussion of each method, a series of example calculations are presented to provide a numerical comparison of the various investigated methods. It should be noted that this analysis and discussion will focus primarily on concrete sleeper track for discussion and example calculations.

Rail seat load calculation methodologies

Inputs to calculations. Three of the most prevalent rail seat load calculation methods that were selected for comparison in this paper are the AREMA method as described in the 2012 Recommended Practices⁸, Talbot's equations for track analysis from the *Railroad Engineering* textbook by William H. Hay¹² and provided in their entirety in the original Talbot Reports¹³, and the Kerr equations from the textbook *Fundamentals of Railway Track Engineering*.¹⁴ Table 1 contains the general equations for the rail seat load for the three methods, as well as what parameters each method includes. Table 2 provides a definition of the variables used in each equation, and a typical magnitude for each parameter.

The variable listed in bold is the notation that will be used for the remainder of this paper, as the notation for the same variable is different for each calculation method. As seen in Table 1, each rail seat calculation method requires certain track characteristics as inputs in order to calculate loads and distributions.

All methods require the applied load as the primary input, generally consisting of the axle or wheel load. Additionally, they all begin with a static load analysis, but only Kerr and Talbot allow the ability to account for dynamic and/or impact loadings of the rail seats from various speeds of train operation. Kerr and Talbot can also account for variability in the support provided by the track structure through inclusion of a track modulus value. A lower track modulus means that the track is essentially less stiff, and more prone to greater deflections under loading. A higher track modulus (i.e. stiffer track) will reduce deflection, but as shown in the calculations presented later in this report, can result in higher rail seat loads.¹⁵ The AREMA manual provides a table of approximate track modulus values for varying sleeper types and support conditions, as shown in Table 3.

In Kerr and Talbot, the sleeper spacing is also an input into the rail seat load calculation. The flexural rigidity of the rail, which is the product of the modulus of elasticity of the rail and the moment of inertia,

Table 1. Rail seat load equations and listing of input parameters.

Dynamic factor	Expression for rail seat load (imperial)	Expression for rail seat load (metric)	Parameters Included					
			Train speed	Wheel diameter	Static wheel load	Sleeper spacing	Modulus of elasticity	Moment of inertia
AREMA ⁸	$(1.5626x + 12.811)P/100$	$(61.52x + 12.811)P/100$			•	•		
Talbot ¹²	$\frac{(P + 0.01 \times P(V - 5)) \times S \times \sqrt[4]{\frac{u}{4EI}}}{2}$	$\frac{(P + 0.01P(0.62V - 5)) \times S \times \sqrt[4]{\frac{10.41u}{EI}}}{.051}$	•		•	•	•	•
Kerr ¹⁴	$\frac{(1 + 0.33 \frac{v}{D}) \times P \times \alpha \times \sqrt[4]{\frac{k}{4EI}}}{2}$	$\frac{(1 + 0.52 \frac{v}{D}) \times P \times \alpha \times \sqrt[4]{\frac{10.41k}{EI}}}{.051}$	•	•	•	•	•	•

Table 2. Rail seat load variable definition.

Variable	Definition	Standard value(imperial)	Standard value (metric)
V, v	Train speed	60 miles/h	96.56 km/h
D	Wheel diameter	36 inches	91.44 cm
u, k	Track modulus	6000 psi	41.37 N/mm ²
x, a, S	Sleeper spacing	24 inches	0.61 m
P	Static wheel load	32,875 pounds	14,912 kg
I	Moment of inertia	93.7 in ⁴	3900 cm ⁴
E	Modulus of elasticity of rail	30,000,000 psi	206,843 N/mm ²

Table 3. Track modulus values for various sleeper configurations (adapted from AREMA⁸).

Sleeper configuration	Track modulus (k, lb/in/in, (n/mm ²))
Wood-sleeper track, after tamping	1000 (6.89)
Wood-sleeper track, compacted by traffic	3000 (20.68)
Plastic composite-sleeper track, compacted by traffic	3000 (20.68)
Concrete-sleeper track, compacted by traffic	6000 (41.37)
Wood-sleeper track, frozen ballast and subgrade	9000 (62.05)
Concrete-sleeper track, frozen ballast and subgrade	18,000 (124.11)

is also an input for some of the calculations. The modulus of elasticity of the rail can vary depending on the material composition of the steel, but is generally considered to be 30,000 ksi (207,000 MPa) for railroad applications. The moment of inertia is dependent on the size of the rail section, and a larger rail section will produce a higher flexural rigidity.

AREMA requires the least number of inputs, and only includes static wheel load and sleeper spacing. The equations for Kerr and Talbot only differ due to the dynamic factor used, as both equations are derived from the theory of a beam on an elastic

foundation. The dynamic factor used in Talbot increases static loads by 1% for every mile/h (1% for every 1.61 km/h) increase in speed above 5 miles/h (8.05 km/h). The dynamic factor used by Kerr accounts for train speed and wheel diameter, and is the only method to use wheel diameter.

Another difference between the Kerr and Talbot methods is the value used for track modulus. Talbot simply uses the recorded value of track modulus for the location to be analyzed. Alternatively, Kerr accounts for the worst-case scenario, stiff ballast during winter months. To estimate the winter modulus, the summer modulus is multiplied by three.

This cannot be seen from Table 1, but is accounted for by the value chosen for u .

In order to develop a more in-depth analytical understanding of how the rail seat load calculated by the various methods changes as critical input parameters are varied, Table 4 contains equations that calculate rail seat load as all but one parameter is held constant. For example, in the train speed column, all variables except train speed are held constant, and then the equation for rail seat load is provided in terms of train speed. The values of each variable used to calculate these equations can be found in Table 2. This table can be used to understand how significant the effect of changing the value of a variable will be on the calculated rail seat load.

Example calculations. In order to numerically compare the various methodologies for calculating rail seat loads, example calculations were performed. A spreadsheet was created for two formats of input load. In one format, the input load is simply a determined applied load value, and no speed factors are involved. This format would be more beneficial to compare with modelling work or field experimentation where a given static load is applied to the rail. Other inputs include sleeper spacing, track modulus, and the selection of 115RE, 132RE, 136RE or 141RE size rail section. For this example calculation, input loads ranging from 10,000 to 50,000 pounds (4540 to 22,700 kg) were used and plotted for each of the four discussed rail seat load calculation methods. A sleeper spacing of 24 inches (0.61 m) was used, the selected rail size was 136RE, and the input track modulus was 6000 lb/in/in (41.4 N/mm²) for concrete sleeper track. Table 5 shows calculated results, and Figure 2 shows them graphically.

The other format of input load is based on rail car weight, and divides the total weight into applied wheel loads. In this format, speed is included as a factor and the dynamic amplification factors available for the Talbot and Kerr equations are calculated based on the value of this input. All other inputs for sleeper spacing, rail size and track modulus are the same as in the previous input format. The three different rail car gross rail loads (GRLs) used as initial input loads are 263,000 lbs (119,402 kg), 286,000 lbs (129,844 kg) and 315,000 lbs (143,010 kg). Table 6 shows the calculated results as well as the respective wheel load for each rail car weight, and Figure 3 is a plot of these results. The speed input for this set of data is 0 mile/h (0 km/h), thus it would simulate a static load from the various train weights. The second set of data is then presented with a 60 mile/h (97 km/h) input in order to compare the effect of speed into these equations versus a static load. These data are shown in Table 7 and plotted in Figure 4.

From these results it can be seen that AREMA initially has the highest predicted rail seat loads.

Table 4. Rail seat load variation according to parameters.

Dynamic factor		Units	Train speed	Wheel diameter	Static wheel load	Sleeper spacing	Moment of inertia	Modulus of elasticity	Track modulus
AREMA ⁸	Imperial (lbs)	16,541	16,541	16,541	0.50P	4211.62 + 513.71S	16541	16,541	16,541
	Metric (kg)	7506	7506	7506	0.50P	1910.38 + 9173.86S	7506	7506	7506
Talbot ¹²	Imperial (lbs)	10,150 + 106.85V	10,150 + 106.85V	16,455	0.50P	688.61S	$611,475 \times \sqrt[4]{\frac{5 \times 10^{-5}}{l}}$	$611,475 \times \sqrt[4]{\frac{16}{E}}$	$611,475 \times \sqrt[4]{\frac{u}{1.12 \times 10^{10}}}$
	Metric (kg)	4575.75 + 29.82V	4575.75 + 29.82V	7466	0.50P	12,240.04S	$276,220 \times \sqrt[4]{\frac{0.0021}{l}}$	$276,220 \times \sqrt[4]{\frac{0.1104}{E}}$	$276,220 \times \sqrt[4]{\frac{u}{7.75 \times 10^7}}$
Kerr ¹⁴	Imperial (lbs)	10,150 + 106.85V	10,150 + 106.85V	$\frac{10,662 + 211.115D}{24,2071}$	0.50P	688.61S	$611,475 \times \sqrt[4]{\frac{5 \times 10^{-5}}{l}}$	$611,475 \times \sqrt[4]{\frac{16}{E}}$	$611,475 \times \sqrt[4]{\frac{u}{1.12 \times 10^{10}}}$
	Metric (kg)	4575.75 + 29.82V	4575.75 + 29.82V	$\frac{4821.18 + 24,2071D}{24,2071}$	0.50P	12,240.04S	$276,220 \times \sqrt[4]{\frac{0.00208}{l}}$	$276,220 \times \sqrt[4]{\frac{0.1104}{E}}$	$276,220 \times \sqrt[4]{\frac{u}{7.75 \times 10^7}}$

Table 5. Rail seat loads for various input load values.

Calculation method	Input load (pounds, (kg))				
	10,000 (4540)	20,000 (9080)	30,000 (13,620)	40,000 (18,160)	50,000 (22,700)
AREMA	5031 (2284)	10,063 (4569)	15,094 (6853)	20,125 (9137)	25,157(11,421)
Talbot	3243 (1472)	6487 (2945)	9730 (4417)	12,973 (5890)	16,217 (7363)
Kerr	4268 (1938)	8537 (3876)	12,805 (5813)	17,074 (7752)	21,342 (9689)

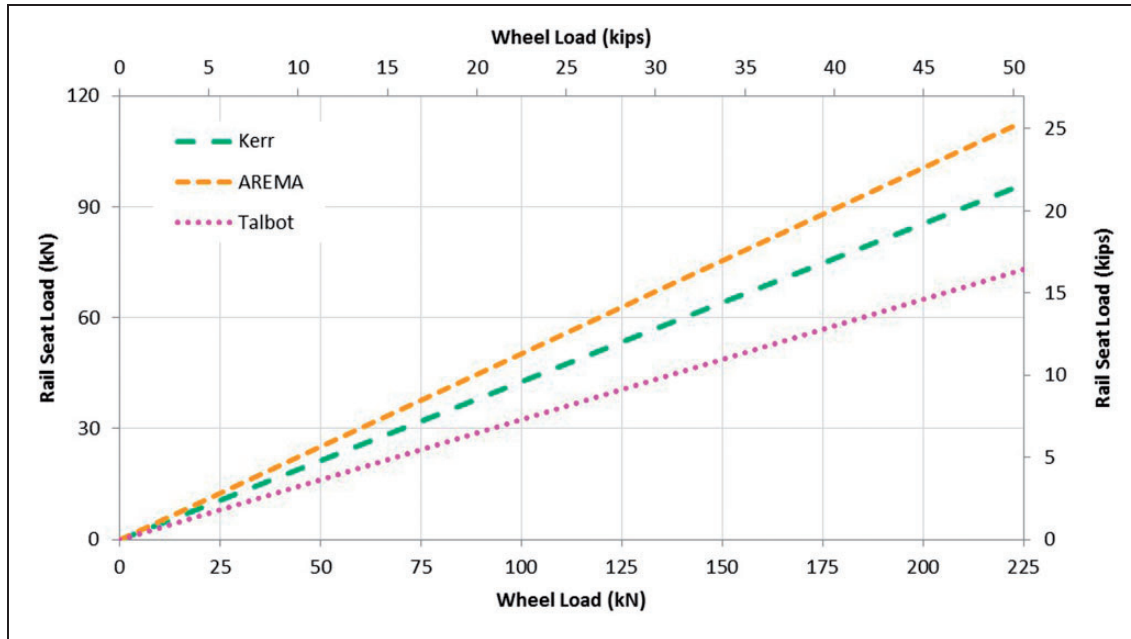


Figure 2. Multiple rail seat load calculation methodologies.

Table 6. Rail seat loads as a function of input loads at rest.

Rail car gross rail load (pounds, (kg))	263,000 (119,402)	286,000 (129,844)	315,000 (143,010)
Wheel load (pounds, (kg))	32,875 (14,925)	35,750 (16,230)	39,375 (17,876)
Calculation method	Calculated rail seat load (pounds, (kg))		
AREMA	16,541 (7510)	17,987 (8166)	19,811 (8994)
Talbot	10,616 (4820)	11,545 (5241)	12,715 (5773)
Kerr	14,032 (6371)	15,260 (6928)	16,807 (7630)

However, because the other methods include some form of a dynamic amplification factor, as speed is introduced into the calculations the values for these three methods are increased. It should be noted that the wheel load values in Table 7 are still based on the weight of the rail car. They may not necessarily represent the actual load applied to the rail by a wheel in this case as dynamic amplification factors are included in the calculations.

Laboratory experimental results

In order to determine which rail seat load calculation methodology most closely predicts field conditions, researchers at UIUC used a full-scale track-loading system (TLS) to measure rail seat loads under realistic loading conditions. The TLS is a full-depth ballast bed that contains 11 sleepers and uses actuators to load a wheel set in order to match the loading

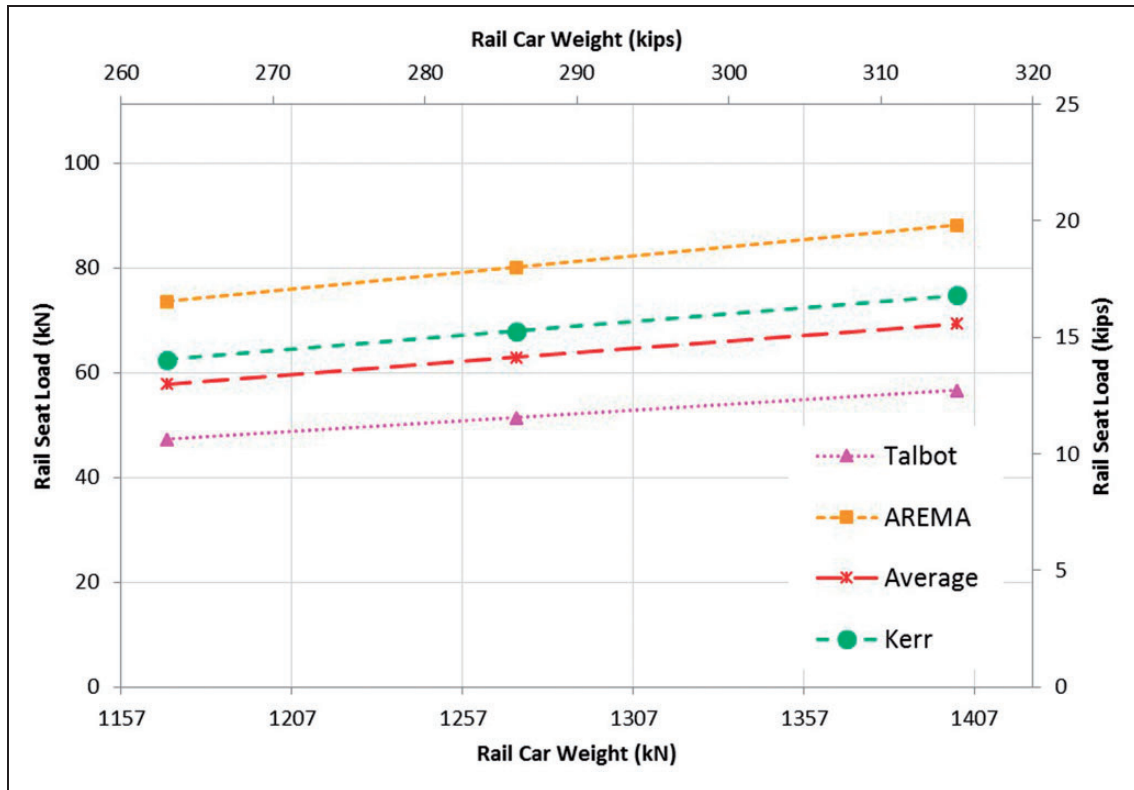


Figure 3. Rail seat loads for various rail car weights at rest.

Table 7. Rail seat loads for various input load values at 60 mile/h (97 km/h).

Rail car gross rail load (pounds, (kg))	263,000 (119,402)	286,000 (129,844)	315,000 (143,010)
Wheel load (pounds, (kg))	32,875 (14,925)	35,750 (16,230)	39,375 (17,876)
Calculation method	Calculated rail seat load (pounds, (kg))		
AREMA	16,541 (7510)	17,987 (8166)	19,811 (8994)
Talbot	16,455 (7471)	17,894 (8124)	19,709 (8948)
Kerr	21,750 (9,875)	23,652 (10,738)	26,051 (11,827)

conditions expected in the field. TLS instrumentation allows for rail seat loads at multiple sleepers to be measured, which can be compared to the predicted values from AREMA, Talbot, and Kerr. Due to the ballast conditions in the TLS, a representative rail seat load for a sleeper with poor, average and good support can be provided. Figure 5 compares the measured rail seat loads to those as predicted by the various analytical methods.

The predictions tend to be overly conservative, as the sleeper with good support exceeded the predicted rail seat loads from all methods by up to 100% at 40 kips (175 kN). For average support, Talbot provides the closest prediction for low wheel loads, whereas AREMA provides the closest prediction for higher rail seat loads.

Field experimental results

In addition to laboratory experimentation, researchers at UIUC instrumented concrete sleepers at the Transportation Technology Center (TTC) in Pueblo, Colorado in order to provide quantitative measurements of rail seat loads under realistic operating conditions. Ten individual concrete sleepers were instrumented with strain gauges in order to measure the rail seat load and wheel load of train consists that passed over the section of track. It was determined that this number of sleepers would provide a reasonable sampling of support conditions, and would accurately capture the inherent sleeper-to-sleeper support variation. A section located in tangent track was used for this comparison in order to provide a

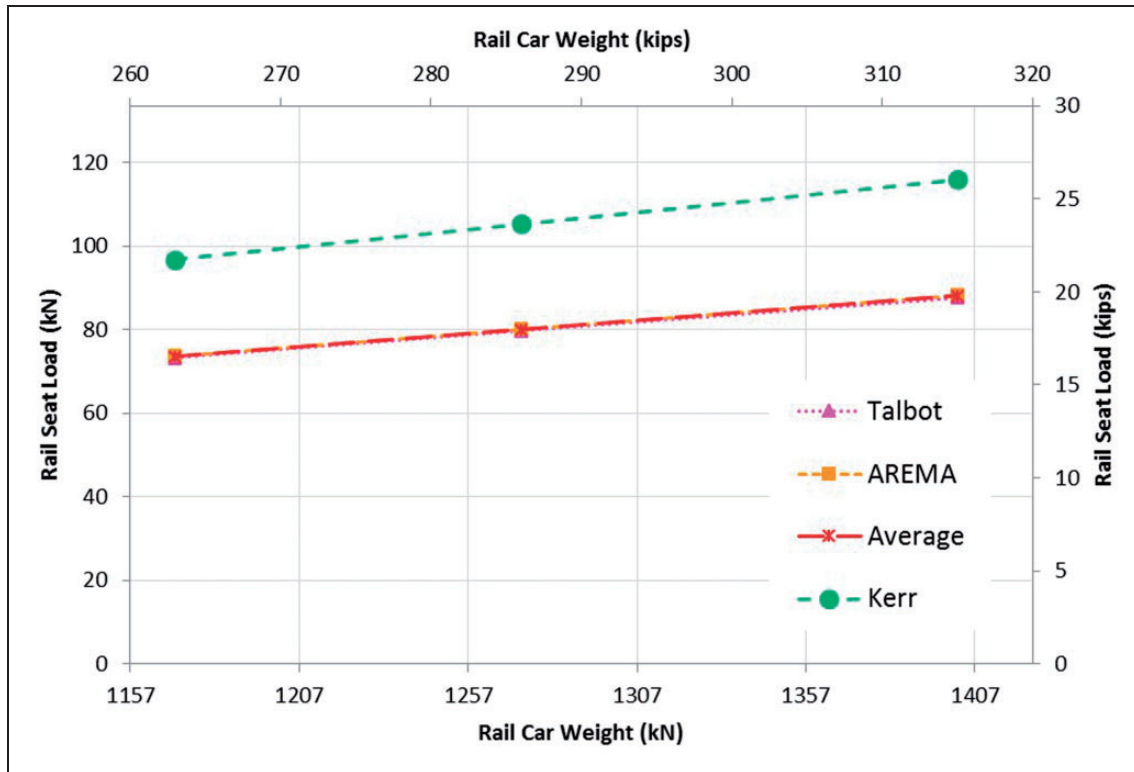


Figure 4. Rail seat loads for various rail car weights at 60 mile/h (97 km/h).

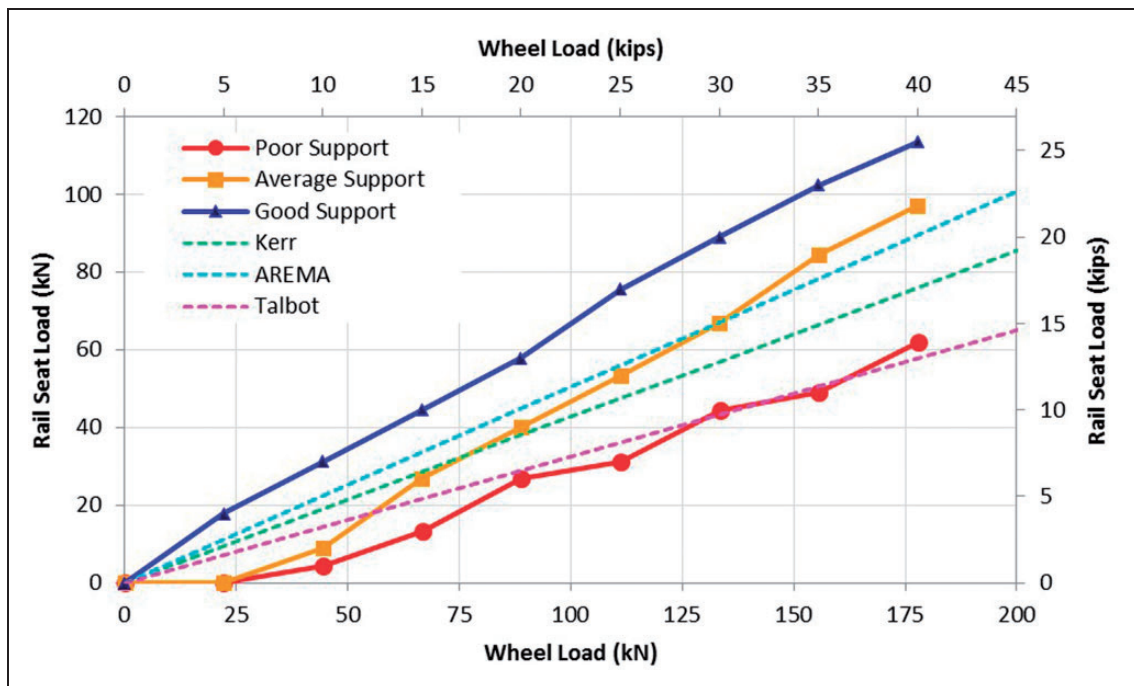


Figure 5. Experimental rail seat load magnitude compared with theoretical calculations.

measurement of rail seat load with minimal lateral load. The train consist used in this study had multiple cars with a maximum GRL of 263,000 lbs (119,295 kg), 286,000 lbs (129,727 kg) and 315,000 lbs (142,882 kg) cars, travelling at a variety of realistic operating speeds. The results from the three rail seat

load calculation methodologies plotted in Figures 6 and 7 were compared to the rail seat loads measured in the field at TTC in order to determine how well the methods predict actual rail seat loads.

Figure 6 compares the rail seat loads for the static case, using data from a train consist travelling at

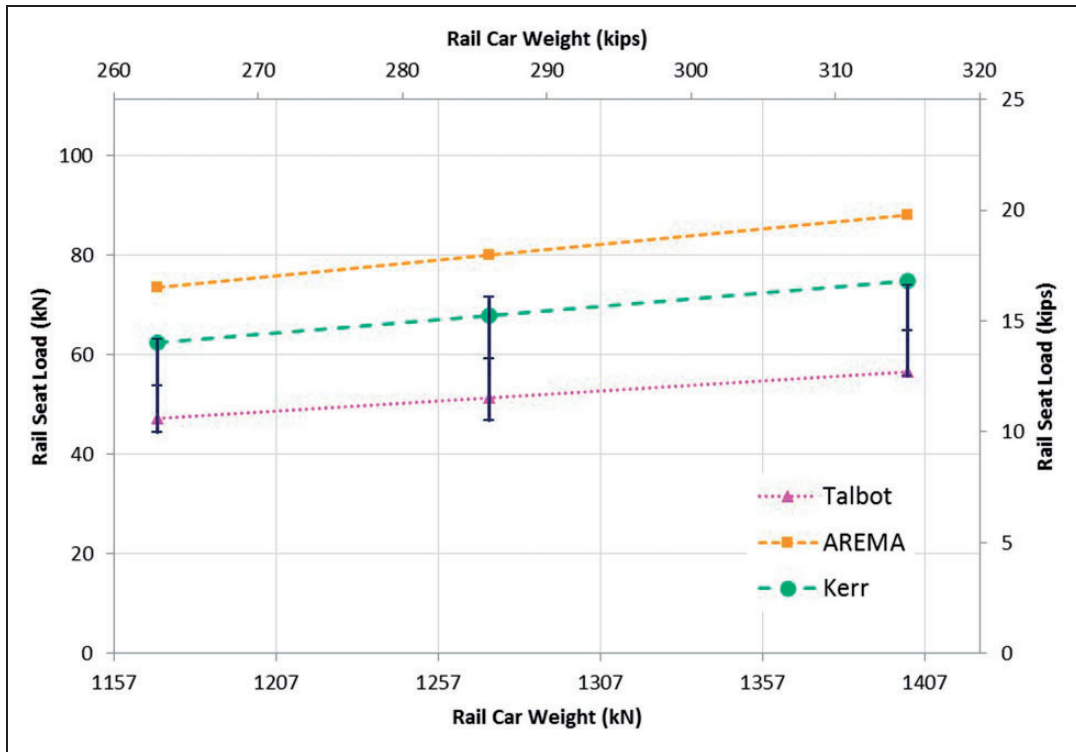


Figure 6. Field rail seat load compared with theoretical calculations - static case.

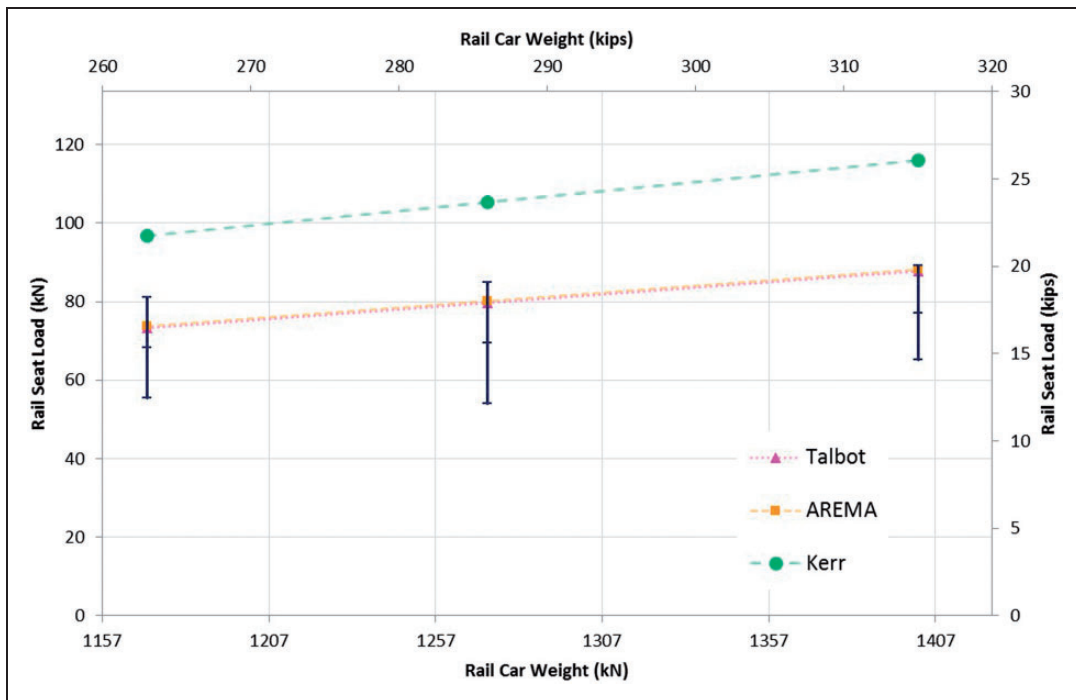


Figure 7. Field rail seat load compared with theoretical calculations – 60 mile/h (96.56 km/h).

2 mile/h (3.2 km/h), widely considered to be a reasonable approximation for a static load. The middle bar represents the mean measured rail seat load for each car weight, whereas the top and bottom bars represent two standard errors (SEs) from the mean. The rail

seat loads measured in the field tended to fall in between the Kerr and Talbot methods, whereas the AREMA method consistently predicted a higher load than was experienced. Since the AREMA method does not account for the increase in rail seat load

due to speed, a high initial prediction would be expected. Each data point was generated from 48, 32 and 64 wheel loads for 263,000 lbs (119,295 kg), 286,000 lbs (129,727 kg) and 315,000 lbs (142,882 kg) cars, respectively.

Figure 7 compares the measured and predicted rail seat loads for a train consist travelling at 60 mile/h (96.56 km/h), a common maximum operating speed for North American freight trains. In this case, the mean recorded rail seat load is lower than all prediction methodologies for all car weights. The predicted rail seat loads for Talbot and AREMA are just barely within two SEs of the measured rail seat loads, whereas the Kerr method is significantly higher than measured for all car weights. These results suggest that the field location had average-to-poor support conditions, resulting in lower rail seat loads than would be expected. Visual inspection of the location, and other data collected at TTC dispute this finding, and point to a stiff subgrade support.

Conclusions

There are various methods for calculating rail seat loads that range from simplified assumptions of the distribution of the wheel load onto the supporting sleepers by the rails, to more complex estimations with the inclusion of several track quality variables. Under static loading conditions, the AREMA method results in maximum rail seats loads. However, when the variable of speed is included, the Talbot and Kerr calculations are increased, as these are the only two methods that present a dynamic amplification factor of some type. The results from the Kerr equation would be identical to those from Talbot, but Kerr uses a higher track modulus to account for frozen ballast. The AREMA method at this input load is approximately 18% higher than Kerr. With the introduction of speed into the equations, for this same wheel load at 60 mile/h (97 km/h), the Kerr method yields a higher value, at approximately 32% higher than the Talbot method. At this speed and wheel load the calculated AREMA value is only 0.5% higher than Talbot, demonstrating the effect of the dynamic factor on the rail seat load in the Talbot equations. The Kerr method uses the most severe dynamic factor, leading it to have significantly higher calculated rail seat loads under high speeds than the other methods.

The methods that are more complex and allow for a wider variety of inputs are able to produce results that more accurately describe rail seat loads with poor and average support. However, all three methods analyzed in this report underestimate the magnitude of rail seat loads as measured by laboratory experimentation for good support conditions. The trends from the data as measured in the field showed the opposite trend, with all three rail seat calculation methods overestimating the magnitude of rail seat load. This emphasizes the

importance of support conditions and its impact on rail seat load. The presented methods can be used to gain a better understanding of the loads seen by individual discrete rail seat areas.

The analytical and experimental methods outlined in this paper contribute to a clearer understanding of how the track structure behaves, providing groundwork for improved design of concrete sleepers and fastening systems. Future work should be aimed at collecting additional experimental data to provide replicates at locations with differing support conditions, with the objective of constructing a model that is capable of accurately calculating rail seat loads given known inputs.

Acknowledgements

Industry partnership and support has been provided by the Transportation Technology Center, Inc.; Union Pacific Railroad; BNSF Railway; National Railway Passenger Corporation (Amtrak); Amsted RPS / Amsted Rail, Inc.; GIC; Hanson Professional Services, Inc.; CXT Concrete Ties, Inc., an LB Foster Company; and TTX Company.

Funding

The author(s) disclosed receipt of the following financial support for the research, authorship, and/or publication of this article: The authors would like to thank the US Department of Transportation (DOT) Federal Railroad Administration (FRA) for providing funding for this project. The published material in this paper represents the position of the authors and not necessarily that of the DOT. J. Riley Edwards has been supported in part by grants to the UIUC and RailTEC from CN, Hanson Professional Services, and the George Krambles Transportation Scholarship Fund.

References

1. Leong J and Murray MH. Probabilistic analysis of train-track vertical impact forces. *Proc Inst Civil Engrs-Transport* 2008; 161(1): 15–21.
2. AS 1085.14: 2003. Australian standard. *Railway Track Material, Part 14: Prestressed Concrete Sleepers*. Sydney: Standards Australia International Ltd.
3. Van Dyk BJ, Dersch MS, Edwards JR, et al. Load characterization techniques and overview of loading environment in North America. *Transport Res Record – J Transport Res Board* 2014; 2448: 80–86.
4. Van Dyk BJ, Dersch MS, Edwards JR, et al. Evaluation of dynamic and impact wheel load factors and their application for design. *Transport Res Record – J Transport Res Board*, accepted 2014.
5. Koch K. *Measurement of wheel load and axle strain environment, 286,000-pound gross rail load coal train service; Powder River Basin to New York, March 2006; Powder River Basin to Georgia, May 2006*. Report R-983, 2007. Pueblo, CO: Association of American Railroads.
6. Kerchof B and Wu H. Causes of rail cant and controlling cant through wheel/rail interface management. In: *The 2012 annual AREMA conference*, Chicago, IL, 16–19 September 2012. Virginia Beach: AREMA, p. 19.
7. Rhodes D and Cox SJ. Rail fastenings for heavy haul and extreme longitudinal forces. In: *The 10th*

- International Heavy Haul Association conference*, New Delhi, India, 4–6 February 2013, pp. 123–126. New Delhi, India: IHHA.
8. American Railway Engineering and Maintenance-of-Way Association. *AREMA manual for railway engineering*. vol 1, Landover, MD: American Railway Engineering and Maintenance-of-Way Association, 2012.
 9. Marquis BP, Muhlinger M and Jeong DY. Effect of wheel/rail loads on concrete tie stresses and rail roll-over. In: *The ASME 2011 Rail Transportation Division fall technical conference*, Minneapolis, MN, 21–22 September 2011, p. 2. New York, NY: ASME.
 10. Kernes RG, Riley Edwards J, Dersch MS, et al. Investigation of the dynamic frictional properties of a concrete crosstie rail seat and pad and its effect on rail seat deterioration (RSD). In: *The 91st annual meeting of the Transportation Research Board*, Washington, DC, 22–26 January 2012, p. 2. Madison, WI: Omnipress.
 11. International Union of Railways. *Design of monoblock sleepers*. Report no.UIC 713C, 2004. Paris, France: UIC.
 12. Hay WH. *Railroad engineering*. Second ed. New York, NY: John Wiley & Sons, 1982.
 13. SK Chambers (ed.) *Stresses in railroad track – the Talbot reports*. Washington, DC: American Railway Engineering Association, 1980.
 14. Kerr AD. *Fundamentals of railway track engineering*. First ed. Omaha, NE: Simmons-Boardman Books, 2003.
 15. Lu S, Arnold R, Farritor S, et al. On the relationship between load and deflection in the railroad track structure. In: *The 2008 Annual AREMA Conference*, Salt Lake City, UT, 21–24 September 2008, p. 2. Virginia Beach, VA: AREMA.